THE JOURNAL OF PHYSICAL CHEMISTRY A

Article

pubs.acs.org/JPCA

Effects of Charge and Substituent on the S···N Chalcogen Bond

Upendra Adhikari and Steve Scheiner*

Department of Chemistry and Biochemistry, Utah State University, Logan, Utah 84322-0300, United States

Supporting Information

ABSTRACT: Neutral complexes containing a S···N chalcogen bond are compared with similar systems in which a positive charge has been added to the S-containing electron acceptor, using high-level ab initio calculations. The effects on both XS···N and XS^+···N bonds are evaluated for a range of different substituents X = CH_3, CF_3, NH_2, NO_2, OH, Cl, and F, using NH_3 as the common electron donor. The binding energy of $XMeS···NH_3$ varies between 2.3 and 4.3 kcal/mol, with the strongest interaction occurring for X = F. The binding is strengthened by a factor of 2−10 in charged $XH_2S^+···NH_3$ complexes, reaching a maximum of 37 kcal/mol for X = F. The binding is weakened to some degree when the H atoms are replaced by methyl groups in $XMe_2S^+···NH_3$. The source of the interaction in the charged systems, like their neutral counterparts, is derived from a charge transfer from the N lone pair into the σ^*(SX) antibonding orbital, supplemented by a strong electrostatic and smaller dispersion component. The binding is also derived from small contributions from a CH···N H-bond involving the methyl groups, which is most notable in the weaker complexes.

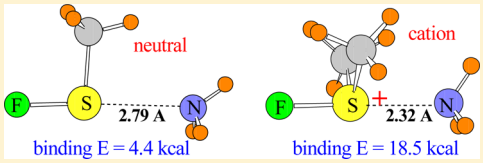

INTRODUCTION

A chalcogen bond is formed when a member of this family of atoms (e.g., S or Se) engages in an attractive and direct noncovalent interaction with an electronegative atom like N or O.[1−15] As such, it is closely related to the halogen[16−25] and pnicogen[26−35] bonds, which have received a great deal of recent attention. There are also parallels with H-bonds (HBs) in that the interaction is at least partly due to a charge transfer from the electron-donor lone pair to a σ^* antibonding orbital of the acceptor; the increased occupation of the latter leads to a lengthening of the corresponding internal bond within the electron-acceptor unit. The importance of chalcogen bonds has been underscored by their strength, which is comparable to and sometimes exceeds that of HBs. For instance, there is a direct interaction of S of FHS with N of NH_3, forming a strong S···N noncovalent bond[36] with a binding energy of 8 kcal/mol.

Just as the electron acceptor can be any of several chalcogen atoms, the electron donor does not have to be N, but also, P, S, or O[37−39] serve as other examples. The transferred charge also does not have to originate in a lone pair, but it can also be extracted from various π-systems including simple double and triple bonds, as well as conjugated and aromatic systems. In such cases, the bonding can be reinforced[37] by back-donation in the reverse direction, from the chalcogen lone pairs into π^* antibonding orbitals. Effects of different substituents X on the XS···N interaction[40] have been recently studied. It was learned that the most electronegative substituents like F and Cl enhance the interaction by the largest amount, just as electron-releasing groups such as CH_3 and NH_2 have the opposite effect. Regardless of the substituent, the components of binding remain the same although induction plays a more dominant role as the complexes are strengthened.

The presence of charge on either of the interacting units has been shown to have a profound effect on HBs. For instance, the water dimer is bound by a OH···O HB with a binding energy of some 5 kcal/mol. However, the presence of either positive or negative charge on one of the H_2O molecules enhances the binding energy[41−43] by a factor of 5−8. Even much weaker HBs are strengthened by a charged subunit. One striking example arises in lysine methyl transferase enzymes where S-adenosylmethionine, containing a sulfonium cation, magnifies the usually weak CH···O HB to the point where it becomes an important part of the enzymatic mechanism.[44] Another recent study shows that the positive charge in trialkyl sulfonium and tetraalkyl ammonium enhances the (S^+/N^+)−CH···O HB energy[45] by a factor of 4−9. The magnifying effect of this charge remains in effect even when the (S^+/N^+) center and the CH groups are separated by a long hydrocarbon chain.

Given the strong effects of charge upon HBs, the obvious question arises as to whether chalcogen bonds are subject to similar changes. There are some indications in the literature that this might be the case. There are a number of indications that halogen bonds that involve an anionic electron donor can be rather strong,[46−54] and similarly for tetrel bonds.[55] Cationic systems are less extensively studied. In one related work, a direct Z···N interaction was preferred over Z−H···N HBs in certain cases[56] where the subunit containing the pnicogen atom Z was positively charged. An ion that does not itself participate in a halogen bond but instead is positioned nearby can nonetheless exert a strengthening influence as well.[57,58] Data for the chalcogen bonds are rare, although a charge-assisted chalcogen bond was identified between chalcogen atoms S and Se and halide anions;[59,60] therefore, there is reason to believe that charge may very well strengthen these bonds. There does

Received: February 10, 2014
Revised: April 4, 2014
Published: April 10, 2014

dx.doi.org/10.1021/jp501449v | J. Phys. Chem. A 2014, 118, 3183−3192

not appear to be anything in the literature dealing with systems in which it is the chalcogen-containing subunit that bears the charge.

The present work is aimed at filling this important gap in our understanding of the chalcogen bond. The S···N interaction is the focus of our attention, particularly the effect of adding a positive charge to the electron-accepting S subunit. After first comparing H_3S^+ with H_2S, the H atoms are replaced by methyl groups, which adds the possibility of a $^+$CH···N HB that could either supplement or compete with the S···N interaction. These methyl groups also serve as a model of the alkyl chains that might be found in the sulfones in certain biological situations. Various substituents X (CH_3, H, NH_2, CF_3, NO_2, OH, Cl, and F) are added to the electron acceptors to examine the combination of substituent effects with charge enhancement.

COMPUTATIONAL METHODS

All calculations were performed using the Gaussian 09 package[61] at the MP2/aug-cc-pVDZ level of theory. This level of theory has been found to be consistent with the so-called gold standard CCSD(T) with larger basis sets and with available experimental quantities, especially for the sorts of systems considered here.[17,28,34,62−69] All minima were verified as having no imaginary frequencies. Binding energies were calculated as the difference in energy between the optimized complex and the sum of energies of separately optimized monomers. Basis set superposition error (BSSE) was removed by the counterpoise correction.[70] Natural bond orbital (NBO) analyses[71,72] were performed to evaluate second-order perturbation energies $E(2)$ using procedures contained within Gaussian within the context of the aug-cc-pVDZ basis set. Symmetry adapted perturbation theory (SAPT)[73] of the Hartree−Fock variety was used to decompose the total binding energy into several components via the Molpro[74] set of codes, also using aug-cc-pVDZ.

RESULTS

Neutral X(Me)S···NH_3 Complexes. Neutral complexes were constructed by permitting X(Me)S to interact with universal electron donor NH_3, with X pointing away from the S···N axis. NH_3 was chosen for this purpose for a number of reasons. In the first place, it has been used extensively for this purpose by our group as well as others, which facilitates comparison between different systems and published reports. Second, its lone pair provides a ready source of electrons. The presence of only a single lone pair avoids geometrical complications that would arise if there were multiple lone pairs. The absence of substituents also avoids secondary interactions that might complicate the analysis of the chalcogen bond. Finally, the small size of this molecule permits higher-level and more accurate calculations to be applied. In addition to the S···N noncovalent bond, the methyl group in the electron acceptor offers a second alternative interaction, namely, a CH···N HB. The fully optimized X(Me)S···NH_3 geometries with various substituents X are presented in Figure 1, along with some of the most important geometrical parameters. The first two rows of Table 1 report the binding energies both without and with counterpoise correction. This quantity increases in the order of X = NH_2 < CH_3 < H < OH < CF_3 < Cl < NO_2 < F and ranges from 2.32 kcal/mol for X = NH_2 to 4.42 kcal/mol for X = F. The S···N distance varies between 2.792 and 3.308 Å. The XS···N arrangement is within 4° of linearity in all cases.

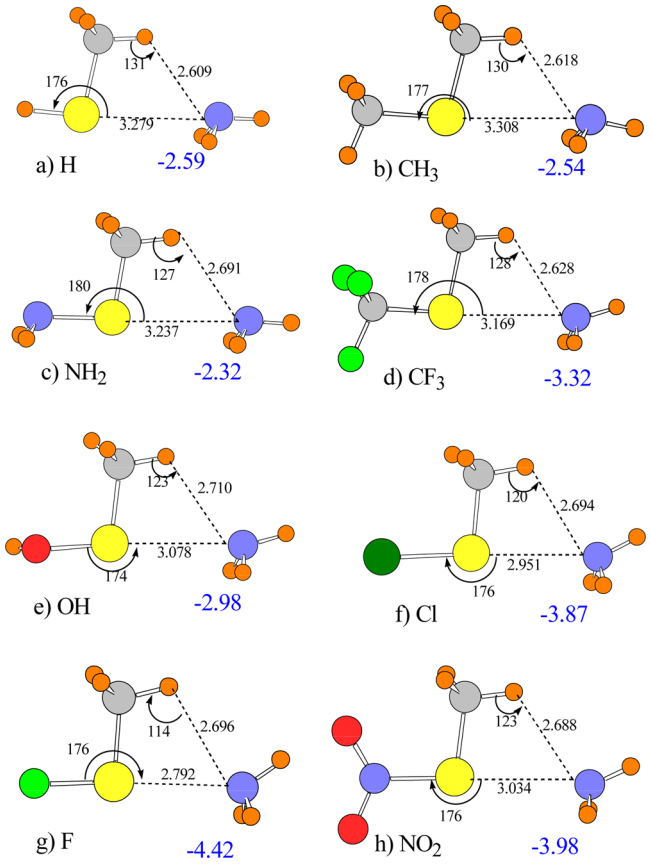

Figure 1. Optimized geometries of X(Me)S···NH_3 complexes for X = (a) H, (b) CH_3, (c) NH_2, (d) CF_3, (e) OH, (f) Cl, (g) F, and (h) NO_2. Distances are in Å, and angles are in degrees. Counterpoise-corrected binding energies in kcal/mol are represented by blue numbers.

As indicated above, these structures are stabilized primarily by two possible attractive forces. Charge transfer from the N lone pair can flow to either the S−X σ^* antibonding orbital or to a methyl C−H σ^*. In either case, this transfer will be accompanied and revealed by a number of factors. Transfer into an antibonding orbital should lengthen the relevant bond, and NBO analysis would quantify this stabilizing force via second-order perturbation energy $E(2)$, as well as the amount of charge transferred Δq and the change in occupancy of the pertinent antibonding orbital Δocc.

These quantities are all presented in Table 1 and exhibit some interesting trends. The binding energies are depicted by the black line in Figure 2. The broken blue line represents $E(2)$ for the S···N interaction, which is very small on the left but grows very rapidly from left to right. The CH···S HB obeys a nearly opposite pattern as $E(2)$ is fairly large on the left side of Figure 2 and diminishes by only a small extent as the total bonding is enhanced (see the red broken curve). These trends in $E(2)$ are echoed by Δq and Δocc (see Table 1). One may conclude that there is a CH···N HB present in all of these complexes that is relatively immune to the nature of X but that the growing strength of the binding in the complex can be traced primarily to the S···N bond.

Comparison with Neutral XHS···NH_3 Complexes. Previous calculations[40] have extracted comparable information

dx.doi.org/10.1021/jp501449v | J. Phys. Chem. A 2014, 118, 3183−3192

Table 1. Energetic (kcal/mol) and Geometrical Properties of X(Me)S···NH_3 Complexes

X	H	CH_3	NH_2	CF_3	OH	Cl	F	NO_2
$-\Delta E$	3.68	3.64	3.55	4.61	4.35	5.29	5.97	5.40
$-\Delta E$ + CC[a]	2.59	2.54	2.32	3.32	2.98	3.87	4.42	3.98
R(S···N), Å	3.279	3.308	3.237	3.169	3.078	2.951	2.792	3.034
θ(XS···N), degs	176	177	180	178	174	176	176	176
Δr(X−S)[b], mÅ	0.19	−0.15	1.24	−1.81	4.80	14.18	17.11	−5.01
$E(2)$ $N_{lp} \rightarrow \sigma^*$(S−X)	0.20	0.06	0.30	0.88	1.63	4.14	8.70	3.25
Δq[c], me	0.31	0.12	0.52	1.61	3.24	9.53	17.54	7.14
Δocc[d], me	0.77	0.65	1.46	0.34	4.35	10.97	18.81	−1.87
R(CH···N), Å	2.609	2.618	2.691	2.628	2.710	2.694	2.696	2.688
θ(CH···N), degs	131	130	127	128	123	120	114	123
Δr(C−H), mÅ	−0.58	−0.49	−1.30	−1.06	−2.50	−3.54	−5.44	−2.75
$E(2)$ $N_{lp} \rightarrow \sigma^*$(C−H)	2.17	1.88	1.58	2.24	1.46	1.37	0.93	1.59
Δq[c], me	2.89	2.53	2.08	3.02	1.87	1.77	1.23	2.08

[a]Counterpoise correction. [b]Change in the X−S bond that accepts charge into σ^* antibonding. [c]Computed as $2(F/\Delta\epsilon)^2$. [d]Change of occupation of the S−X σ^* orbital.

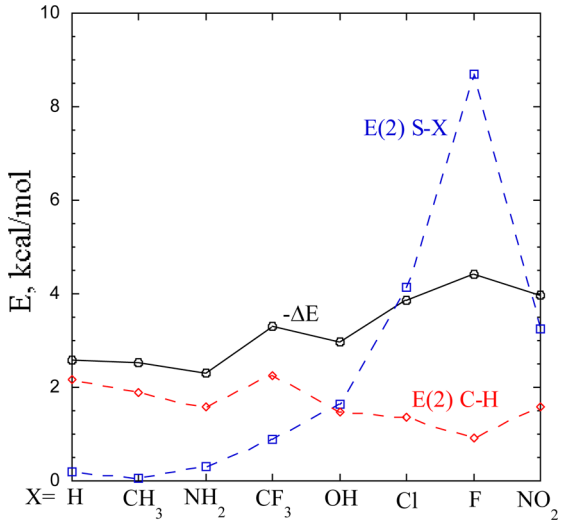

Figure 2. Total binding energies $-\Delta E$ and NBO values of $E(2)$ for X(Me)S···NH_3 complexes. E(2)(S−X) refers to $N_{lp} \rightarrow \sigma^*$(SX) and $E(2)$(C−H) to $N_{lp} \rightarrow \sigma^*$(CH).

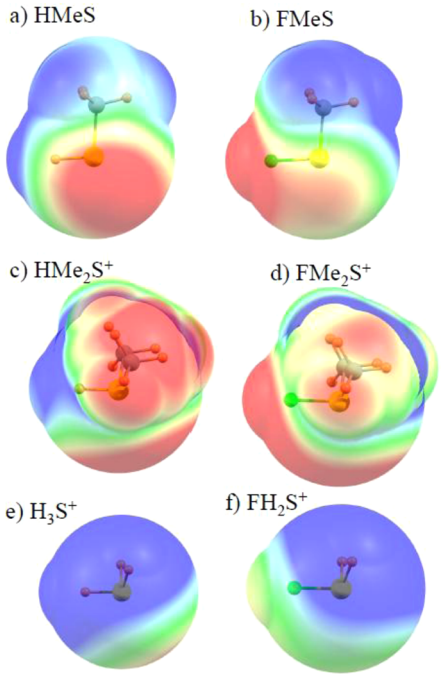

Figure 3. Electrostatic potential maps of monomers (a) HMeS, (b) FMeS, (c) HMe_2S^+, (d) FMe_2S^+, (e) H_3S^+, and (f) FH_2S^+ on a surface lying twice the vdW radius of each atom. Red and blue regions of (a) and (b) indicate −0.015 and +0.015 au, respectively, while they refer to +0.015 and +0.018 au in the cations in (c−f).

for complexes wherein the methyl group is replaced by the simpler H atom. The optimized geometries are similar to those in Figure 1, with some small differences. For one thing, the R(S···N) distances are a bit shorter for XHS···NH_3, and the binding energies are somewhat larger, particularly for the more strongly bound complexes on the right side of Table 1. Given the fact that the methyl groups provide a second binding option of a CH···N as well as a S···N bond, this distinction might seem contradictory. The underlying source of this difference may be traced to the electrostatic potentials of the XHS versus XMeS subunits. Whereas the major lobe of the positive region around XHS lies directly along the X−S axis, this lobe is redirected more toward the methyl group in XMeS, as illustrated in Figure 3a and b for X = H and F, respectively. It is for this reason that the C_3 axis of the NH_3 molecule, corresponding to the N lone pair, is turned up toward the methyl group in most of the structures of Figure 1, whereas this lone pair is more closely aligned with the S···N axis[40] for XHS complexes. This misalignment in the XMeS geometries results in a reduced charge-transfer energy from the N lone pair to the SX σ^* orbital. For example, while $E(2)$ for $N_{lp} \rightarrow \sigma^*$(S−X) ranges to as high as 28 kcal/mol for FHS···NH_3, the corresponding quantity in FMeS···NH_3 is only 9 kcal/mol. The additional $E(2)$ for the CH···N HB in FMeS···NH_3 cannot compensate for this difference as it only amounts to about 1 kcal/mol. As a consequence, the interaction energy in FMeS···NH_3 is only about half of that in FHS···NH_3. The importance of the different electrostatic potentials of FHS and FMeS is verified by a decomposition of the interaction energies in the two corresponding complexes in that the electrostatic component of FMeS···NH_3 is only about half of that of FHS···NH_3.

XH_2S^+···NH_3 Complexes. Adding a proton to each of the XHS subunits leads to a positively charged XH_2S^+ and facilitates an examination of the effect of such a charge upon the properties of the various complexes. The optimized geometries in Figure 4 show that the X substituent lies some 162−171° from the N atom, very similar to their neutral XHS···

dx.doi.org/10.1021/jp501449v | J. Phys. Chem. A 2014, 118, 3183−3192

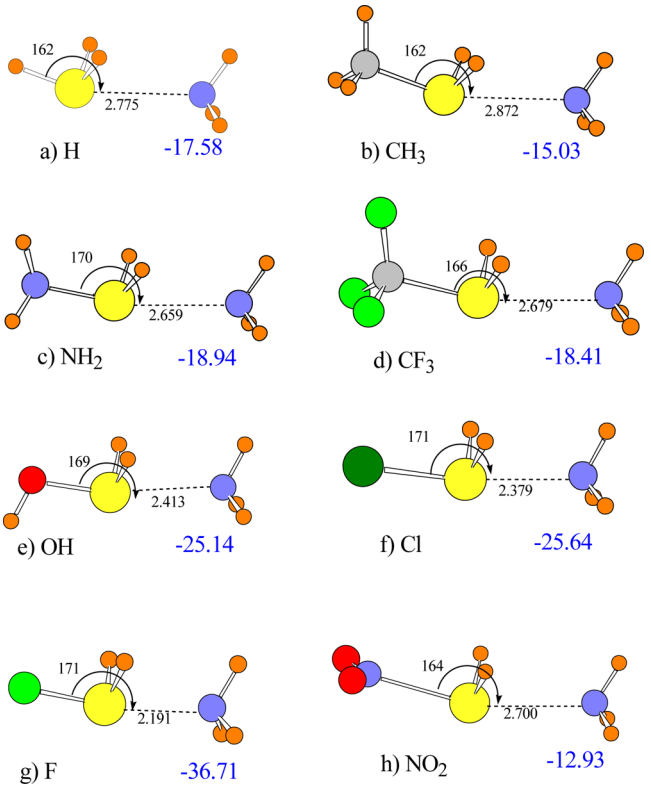

Figure 4. Optimized geometries of $XH_2S^+\cdots NH_3$ complexes for X = (a) H, (b) CH_3, (c) NH_2, (d) CF_3, (e) OH, (f) Cl, (g) F, and (h) NO_2. Distances are in Å, and angles in degrees. Counterpoise-corrected binding energies in kcal/mol are represented by blue numbers.

NH_3 analogues. On the other hand, the charged complexes are much more strongly bound. Whereas the binding energies of the neutrals vary[40] from 1.5 to 7.9 kcal/mol, the charged complexes range between a minimum of 12.9 up to 36.7 kcal/mol. On the weaker side of the spectrum, neutral H_2S does not form a true minimum to NH_3 bound by a S···N bond. In contrast, H_3S^+, H_2MeS^+, and HMe_2S^+ all engage in a strong bond of this type, bound by 17.6, 15.0, and 12.7 kcal/mol, respectively. The latter charged S···N bonds are stronger than any of the neutral analogues. On the strong end, the neutral FS···N bond of 7.9 kcal/mol is magnified by a factor of 4.6 when charged. This magnification is even more pronounced for X = NH_2 and CH_3, where the charged complex is bound more strongly than the neutral system by a factor of 8 and 10, respectively.

Table 2 reports the various energetic and geometric properties of the charged complexes, where it may be observed that the R(S···N) distance varies from 2.19 to 2.87 Å, as compared to the 2.47−3.25 Å range for the neutrals, a charge-induced contraction of roughly 0.3 Å. The $N_{lp} \rightarrow \sigma^*$(SX) charge transfer is also enhanced, with $E(2)$ varying from a minimum of 6.8 kcal/mol up to more than 66 kcal/mol. One notes also large charge transfers as measured both by Δq and Δocc, both up around 150−170 me for the stronger bonds. The charge transfer into the antibonding S−X orbital lengthens this bond in most cases, by as much as 66 mÅ. (Exceptions are discussed below.)

Given the fact that a positive charge would enhance the acidity of the XSH_2^+ species, it might be tempting to suggest that there are $SH^+\cdots N$ HBs present in these ionic complexes that add to the binding energy. However, the R(H···N) distances are rather long, all exceeding 2.4 Å, and the θ(SH···N) angles very far from linearity. The NH_3 molecule also does not rotate its lone pair up toward the SH protons to any significant degree. The absence of significant NBO $E(2)$ values for $N_{lp} \rightarrow \sigma^*$(SH) further confirms the absence of any such HBs.

SAPT decomposition of the ionic $XH_2S^+\cdots NH_3$ complexes reported in Table 3 shows a strong enhancement in each of the components when compared to the neutrals. For example, ES for the neutrals[37] ranged up to a maximum of −24 kcal/mol in $FHS\cdots NH_3$, and this same quantity is equal to −64 kcal/mol for $FH_2S^+\cdots NH_3$. The induction energy is even more enlarged, from −34[37] to −109 kcal/mol. Indeed, whereas ES and IND are roughly equal for the neutral complexes, the latter quantity exceeds ES for the more strongly bound cationic systems by a sizable margin. Even though DISP is enhanced by the charge, it remains considerably smaller than the two other components mentioned above, roughly 15−30% of their magnitudes. SAPT decompositions for all complexes are displayed in Tables S1−S3 of the Supporting Information. It may be seen that the same enhancement effects are observed as well for the methyl-substituted complexes.

$X(Me)_2S^+\cdots NH_3$ Complexes. Evaluation of $X(Me)_2S^+$ as an electron acceptor may be considered in one of two ways. It may be thought of as either the addition of a positive charge to XMeS or as the replacement of the two H atoms of XH_2S^+ by methyls, with no change in charge state. The optimized $X(Me)_2S^+\cdots NH_3$ complexes are illustrated in Figure 5, with other details provided in Table 4. Comparison with Figure 4 and Table 2 reveals first that the replacement of the H atoms of XH_2S^+ by methyls weakens the S···N bond by a surprising amount. For example, the binding energy of $FH_2S^+\cdots NH_3$ is cut in half by this disubstitution, although the diminutions in the other systems are less dramatic. Along with this weakening, there is a concomitant stretch of the R(S···N) distance by some 0.2−0.3 Å, and the θ(XS···N) angle becomes a bit more linear.

Table 2. Energetic (kcal/mol) and Geometrical Properties of $XH_2S^+\cdots NH_3$ Complexes

X	H	CH_3	NH_2	CF_3	OH	Cl	F	NO_2
$-\Delta E$	18.87	16.24	20.65	20.03	27.29	28.00	39.44	14.35
$-\Delta E$ + CC	17.58	15.03	18.94	18.41	25.14	25.64	36.71	12.93
R(S···N), Å	2.775	2.872	2.659	2.679	2.413	2.379	2.191	2.700
θ(XS···N), degs	162	162	170	166	169	171	171	164
Δr(X−S), mÅ	4.3	−6.0	11.8	−30.7	35.1	66.1	65.9	−156.3
$E(2)$ $N_{lp} \rightarrow \sigma^*$(S−X)	6.82	5.06	13.00	10.77	31.15	36.12	66.60	18.58
Δq, me	12.4	9.3	23.8	23.9	61.5	87.3	148.6	97.7
Δocc, me	22.08	15.36	38.1	8.49	88.34	110.44	166.63	−173.46

dx.doi.org/10.1021/jp501449v | J. Phys. Chem. A 2014, 118, 3183−3192

Table 3. SAPT Energy Decomposition (kcal/mol) for the $XH_2S^+\cdots N$ Interaction

	ES	EX	IND	IND+EXIND	DISP	DISP+EXDISP	tot
H	−23.65	15.40	−18.18	−5.35	−4.04	−3.22	−16.81
CH_3	−19.73	12.50	−13.45	−3.98	−3.9	−3.12	−14.33
NH_2	−26.91	21.06	−24.76	−6.39	−5.37	−4.22	−16.45
CF_3	−26.98	20.58	−24.24	−6.71	−5.14	−4.04	−17.15
OH	−41.02	41.52	−53.02	−13.00	−8.03	−6.14	−18.62
Cl	−43.81	48.24	−59.83	−14.90	−8.87	−6.76	−17.22
F	−64.27	75.86	−109.34	−29.30	−11.50	−8.75	−26.41
NO_2	−23.76	21.62	−22.43	−5.91	−5.56	−4.32	−12.37

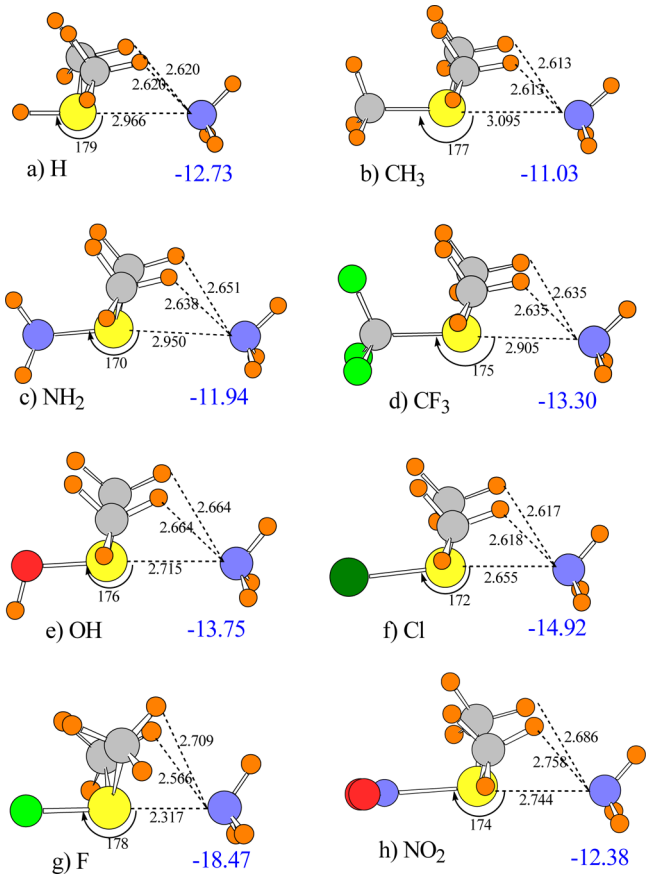

Figure 5. Optimized geometries of $X(Me)_2S^+\cdots NH_3$ complexes for X = (a) H, (b) CH_3, (c) NH_2, (d) CF_3, (e) OH, (f) Cl, (g) F, and (h) NO_2.

There is a sizable drop in the $N_{lp} \rightarrow \sigma^*(SX)$ charge transfer, as measured by $E(2)$, Δq, and Δocc, as well as a diminished S−X bond stretch. (A primary reason for the reduction in molecular interaction strength arising from methyl substitution is elaborated on below.)

Unlike XH_2S^+, the methyl groups of $X(Me)_2S^+$ extend toward the N atom, to the point where they seem capable of forming $SCH^+\cdots N$ HBs, albeit weak ones. The characteristics of these HBs are listed in the lower portions of Table 4, where bond lengths are in the range of 2.6−2.7 Å. The θ(CH···N) angles are substantially distorted from linearity, but there is nonetheless significant $N_{lp} \rightarrow \sigma^*(CH)$ charge transfer, as is evident by $E(2)$, Δq, and a contraction of r(CH), which is characteristic of many CH···N HBs. Although generally weaker than the complexes with XH_2S^+, these $X(Me)_2S^+$ ions form much stronger interactions with NH_3 than do their neutral XMeS counterparts, by a factor of 3−5, with corresponding increases in the various indicators of charge transfer from NH_3 to σ^*(S−X). It is intriguing to note that despite the positive charge on the proton donor $X(Me)_2S^+$, there is what would appear to be a weakening of the CH···N HBs relative to neutral XMeS, in terms of $E(2)$ and Δq, as well as geometrical indicators R(H···N) and θ(CH···N). In summary, the addition of positive charge on the S-electron acceptor very substantially strengthens the S···N bond, at the expense of a small reduction in CH···N HB strength.

In terms of accuracy, one may always question the validity of a given level of theory. As mentioned earlier, the MP2/aug-cc-pVDZ level has proven its fidelity on a number of occasions in the past. In order to check its accuracy on the particular systems examined here, correlation was included via the CCSD(T) approach, using the larger aug-cc-pVTZ basis set for a representative sampling of systems. As may be seen in Table 5, complexes were chosen that were both neutral and cationic, methylated and unmethylated, using both H and F as the two substituents, which represent opposite extremes of binding strength. The comparisons in Table 5 make it clear that there is little difference between the MP2/aug-cc-pVDZ and CCSD(T)/aug-cc-pVTZ binding energies. Values are all within 7% of one another, some differences less than 1%.

Competition between CH···N and S···N interactions. As described above, the CH_3 groups in X(Me)S and $X(Me)_2S^+$ units offer the N lone pair an alternative with which to interact. That is, this lone pair may donate charge to the S−X σ^* orbital in a S···N bond or may interact instead with a CH bond of a methyl group, donating charge into its σ^*(CH) antibonding orbital. The orientation of the NH_3 molecule is heavily influenced by this competition as the former is favored when the lone pair of NH_3 lies along the S···N axis, while a displacement upward toward a methyl group would facilitate the CH···N HB. One can measure this displacement with the simple assumption that the lone pair is collinear with the C_3 symmetry axis of NH_3.

For complexes without methyl groups, XH_2S^+ and neutral XHS, in which there is no CH···N bond, the lone pair lies within 6−9° of the S···N axis. In contrast, the methylated systems vividly illustrate the competition between the S···N and CH···N interactions. For those complexes containing the neutral X(Me)S, the N lone pair is displaced from S···N by a large amount, 66° for HMeS, facilitating the CH···N bond. However, as the substituent becomes progressively more electron-withdrawing and as the S···N interaction strengthens, this deviation diminishes, dropping down below 30° for FHS···NH_3 and 18° for FMeS···NH_3. A similar pattern is observed in the dimethyl FMe_2S^+ cases, although these deviations are systematically smaller here. These angular characteristics affirm the idea that CH···N HBs outweigh S···N for the more weakly

dx.doi.org/10.1021/jp501449v | J. Phys. Chem. A 2014, 118, 3183−3192

Table 4. Energetic (kcal/mol) and Geometrical Properties of $X(Me)_2S^+\cdots NH_3$ Complexes

X	H	CH_3	NH_2	CF_3	OH	Cl	F	NO_2
$-\Delta E$	14.45	12.71	13.93	15.34	16.24	17.50	22.02	14.57
$-\Delta E$ + CC	12.73	11.03	11.94	13.30	13.75	14.92	18.47	12.38
R(S···N), Å	2.966	3.095	2.950	2.905	2.715	2.655	2.317	2.744
θ(XS···N), degs	179	177	170	175	176	172	178	174
Δr(X−S), mÅ	2.3	2.3	10.9	−5.0	22.9	37.3	57.6	−196.3
$E(2)$ $N_{lp} \rightarrow \sigma^*$(S−X)	3.25	1.99	4.06	4.66	12.05	14.55	46.77	13.93
Δq^d, me	5.7	3.6	7.3	9.9	23.6	34.3	97.5	43.0
Δocc^e, me	7.25	3.99	7.87	−79.92	25.54	35.91	96.85	−140.12
R(CH···N)^a, Å	2.620	2.613	2.638	2.635	2.664	2.617	2.566	2.686
θ(CH···N), degs	120	123	117	118	107	109	97	112
Δr(C−H), mÅ	−2.4	−2.2	−4.3	−2.9	−5.5	−5.6	−8.3	−3.7
$E(2)$ $N_{lp} \rightarrow \sigma^*$(CH)	1.17	1.32	0.99	1.00	0.47	0.62	0.73	0.66
Δq, me	1.54	1.73	1.09	1.36	0.61	0.87	1.04	0.88
R(CH···N)^a, Å	2.620	2.613	2.651	2.635	2.664	2.618	2.709	2.758
θ(CH···N), degs	120	123	116	118	107	109	86	105
Δr(C−H), mÅ	−2.4	−2.2	−2.7	−2.9	−5.5	−5.6	−6.9	−3.6
$E(2)$ $N_{lp} \rightarrow \sigma^*$(CH)	1.17	1.29	0.84	1.00	0.47	0.62	0.21	0.49
Δq, me	1.54	1.73	1.36	1.36	0.61	0.87	0.30	0.68

^{a}For two different CH_3 groups.

Table 5. Counterpoise-Corrected Binding Energies (kcal/mol) of Some Representative Complexes with NH_3 Computed at the CCSD(T)/aug-cc-pVTZ Level of Theory^a

	$-\Delta E$ + CC, kcal/mol							
	XHS		XH_2S^+		XMeS		XMe_2S^+	
X	CCSD(T)	MP2	CCSD(T)	MP2	CCSD(T)	MP2	CCSD(T)	MP2
H	1.58	1.47	18.42	17.58	2.79	2.59	13.20	12.73
F	7.52	7.92	36.77	36.71	4.14	4.42	17.99	18.47

^{a}MP2/aug-cc-pVDZ values are shown for comparison.

bound complexes, but it is S···N that dominates as the interaction grows in strength.

Another important factor in controlling the NH_3 orientation is the electrostatic potential around the electron-acceptor molecule. Besides acting as the principal source of electron density for transfer, the NH_3 lone pair is also coincident with the most negative potential around this molecule. As such, this lone pair should be drawn toward the most positive region of the potential around the partner molecule. As was mentioned earlier, the replacement of a H atom in XHS by a methyl group brings the most positive region of the electrostatic potential up toward the methyl group and with it the N lone pair. This upward displacement of the most positive portion of the potential for both HMeS and FMeS is evident by the blue regions in Figure 3a and b. When a second methyl group is added, leading to the XMe_2S^+ cations, however, the displacement is much smaller in that the blue regions in Figure 3c and d lie nearer to the S···N axis, resulting in the smaller upward rotations of the NH_3 molecule in these dimethylated systems, none of which are more than 20°.

The electrostatic potentials also offer a ready explanation for the drop in binding energy when XH_2S^+ is replaced by its dimethylated XMe_2S^+ analogue. Comparison of Figure 3c with e shows a strong increase in the positive electrostatic potential to the right of the S atom when the methyl groups of HMe_2S^+ are both replaced by H. This same effect arises when the F atom is the substituent, as in Figure 3d and f.

The shifts of electron density that accompany the formation of a complex can frequently provide insights about the nature of the interaction. These shifts are displayed in Figure 6 as the difference in density between the complex on one hand and the sum of isolated monomers on the other hand, in the same positions as those in the complex. Purple areas indicate an increased density in the complex, and losses are represented by the green regions. Focusing first on the neutral complexes of Figure 6a and b, both complexes show a purple gain of density in the region of the N lone pair. The green loss around the methyl proton in Figure 6a is characteristic of HBs. (There is

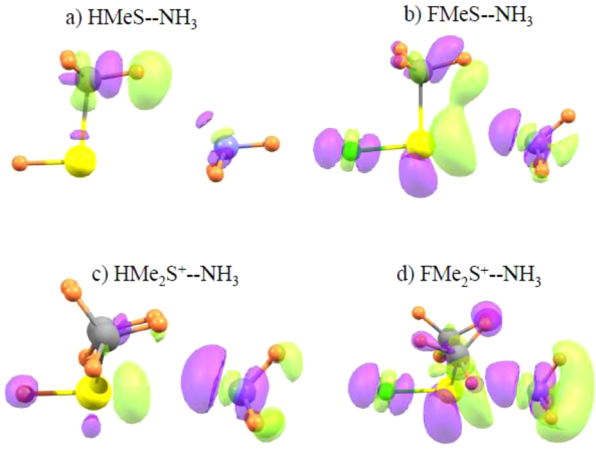

Figure 6. Electron density shifts occurring upon complexation of NH_3 with (a) HMeS, (b) FMeS, (c) HMe_2S^+, and (d) FMe_2S^+. Purple and green regions indicate gain and loss of density, respectively, in dimers relative to monomers. The 0.001 au contour is depicted in a and (b), and the 0.002 au is in (c) and (d).

dx.doi.org/10.1021/jp501449v | J. Phys. Chem. A 2014, 118, 3183−3192

no such density loss around the SH proton of the unmethylated counterparts, verifying the absence of a SH···N HB.) One may note the absence of a green region to the right of S in Figure 6a, consistent with the idea that MeHS is bound to NH_3 primarily by a CH···N HB. The green density-loss region encompasses both the S and CH proton in FHS···NH_3 in Figure 6b, verifying the growing strength of the S···N bond. A gain of density appears also around the F substituent, consonant with the idea of charge transfer into the S−F σ^* orbital.

It is immediately clear that there is much greater density rearrangement in the charged complexes in Figure 6c and d than in their neutral counterparts. (Note also the larger value of the isocontour used for the ionic complexes.) This enhancement is consistent with the stronger binding in the ionic complexes and the idea that a charged species can more powerfully affect the charge distribution within its partner. In these ionic complexes, the green charge-loss region to the right of S dwarfs any density changes around the CH protons, further attesting to the dominance of S···N over CH···N interactions in charged dimers.

Anomalous Behavior of NO_2 and CF_3 Substituents. The reader has probably noticed that complexes containing the NO_2 group have behaved differently than most of the others. For example, the last column of Table 1 shows that even though there is a sizable charge transfer into the S−N σ^* orbital of (NO_2)MeS···NH_3, the net occupancy of this orbital drops by 2 me, and the S−N bond shortens by 5 mÅ; these anomalous effects are magnified in the ionic $(NO_2)H_2S^+$···NH_3 and $(NO_2)Me_2S^+$···NH_3 complexes in Tables 2 and 4, respectively. Indeed, similar contrary behavior, albeit not as large in magnitude, is observed for the $-CF_3$ substituent. The anomalous behavior cannot be attributed to any conformational change within the monomer in question as the overall geometry remains unchanged upon complexation.

What these two substituents have in common is the presence of more than one non-hydrogen atom, and it would appear that it is this feature that permits this counterintuitive behavior. In particular, charge is indeed transferred from the N lone pair to the S−N σ^* antibonding orbital of $(NO_2)H_2S^+$, as is evident from the NBO analysis. However, this charge does not remain there, continuing on to the O lone pairs in the case of NO_2. Not only this charge but also a certain amount of density that originally resided in the N−S σ^* orbital in the monomer moves over to the O lone pairs as well, making the O atoms more negatively charged. The net decrease in σ^* population is reflected in the values of Δocc, as well as the shortening of the S−N bond. These same principles are in operation within the $-CF_3$ substituent wherein charge is transferred from the S−C σ^* antibonding orbital to the F lone pairs. In both the NO_2 and CF_3 substituent cases, the increased density in the peripheral atom lone pairs is visible when viewing the density difference maps.

SUMMARY

The effects of methylation and of addition of a charge are summarized in Figure 7, which displays the total binding energy for the four sorts of systems and how this quantity varies as the substituent is changed. For each type of interaction, whether neutral or charged, the interaction grows stronger as the substituent becomes more electron-withdrawing (with the exception of X = NO_2). The two neutral types containing either XHS or XMeS are generally similar to one another, although the former is a bit stronger for the more electro-

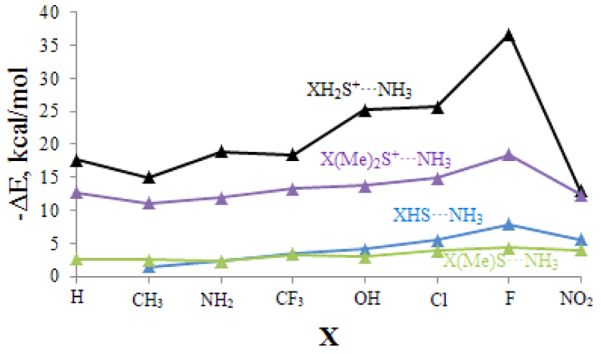

Figure 7. Variation of the binding energy (kcal/mol) of neutral and cationic S···N complexes with various substituents.

negative groups on the right side. The ionic complexes are much more strongly bound, in particular, XH_2S^+. For example, FH_2S^+···NH_3 is bound by some 37 kcal/mol, which represents a nearly 5-fold magnification compared to its neutral FHS···NH_3 analogue. Accompanying this charge-induced strengthening is a reduction in the intermolecular separation by some 0.5 Å on average.

The total binding energy is strongly correlated with the charge transfer from the N lone pair into the S−X σ^* antibonding orbital, as verified by a number of markers, including $E(2)$, the change in occupation of the σ^* orbital, and the stretch of the S−X bond length. For example, the correlation coefficient relating $E(2)$ to the binding energy is equal to 0.91 for complexes involving XMeS, 0.94 for XMe_2S^+, and 0.80 for XH_2S^+. The induction energy is comparable to, and in some cases larger than, the electrostatic interaction energy. The dispersion energy is considerably smaller but cannot be ignored, amounting to as much as 11 kcal/mol in the most strongly bound system.

In addition to the S···N bond, there is a certain amount of CH···N H-bonding involving a methyl group on the S atom. This bond makes a fixed, but small, contribution to the total interaction energy, fairly insensitive to the nature of other substituents on the S. Consequently, the weakest complexes rely to a large degree on the CH···N HB for their stability, whereas it is S···N that predominates for the stronger complexes. On the other hand, the replacement of a H atom on S by a methyl group displaces the positive portion of the electrostatic potential of the monomer away from the S atom. This displacement tends to draw the NH_3 lone pair away from the S−X σ^* orbital, thereby weakening the interaction.

The NO_2 substituent behaves somewhat differently than the other substituents in that the charge that the monomer acquires from the NH_3 lone pair does not remain in the σ^* S−N antibonding orbital but continues on into the O lone pairs. It is for this reason that the S−N bond contracts and the O atoms become more negatively charged. This anomalous behavior also accounts for the drop in binding energy for the NO_2 substituent in comparison to those of comparable electron-withdrawing potency (see Figure 7).

It might be noted that not all of the minima studied here represent the global minimum on the corresponding potential energy surface. The OH substituent, for example, is such a strong proton donor that a OH···N HB will typically be energetically preferable to a S···N interaction, and because NH_3 is a more powerful proton acceptor than is XHS, an additional proton would prefer the former site, resulting in an

dx.doi.org/10.1021/jp501449v | J. Phys. Chem. A 2014, 118, 3183−3192

$XHS\cdots{}^{+}NH_4$ complex, rather than $XH_2S^{+}\cdots NH_3$. However, all of the structures considered here represent true minima nonetheless. The need to study complexes of this type is underscored by examples of biological systems where a sulfonium cation is an essential component in the mechanism of certain enzymes. Systems such as these also illustrate the importance of replacing SH protons by a methyl group in the model systems to better represent these biological situations.

In summary, the cationic $S^{+}\cdots N$ interaction represents a very strong force, several-fold greater than its neutral counterparts or uncharged hydrogen and halogen bonds. The addition of a charge does not fundamentally alter the nature of bonding, affecting primarily the magnitudes of the components, nor does the charge alter the ratio of electrostatic and induction components of the total interaction energies.

■ ASSOCIATED CONTENT

Supporting Information

SAPT dissections of complexes and optimized coordinates of complexes. This material is available free of charge via the Internet at http://pubs.acs.org.

■ AUTHOR INFORMATION

Corresponding Author

*E-mail: steve.scheiner@usu.edu.

Notes

The authors declare no competing financial interest.

■ ACKNOWLEDGMENTS

This work has been supported by NSF-CHE-1026826. U.A. is grateful to Utah State University for a Dissertation Award. Computer, storage, and other resources from the Division of Research Computing in the Office of Research and Graduate Studies at Utah State University are gratefully acknowledged.

■ REFERENCES

(1) Bauzá, A.; Quiñonero, D.; Deyà, P. M.; Frontera, A. Halogen Bonding versus Chalcogen and Pnicogen Bonding: A Combined Cambridge Structural Database and Theoretical Study. *CrystEngComm* **2013**, *15*, 3137−3144.

(2) Wang, X.-Y.; Jiang, W.; Chen, T.; Yan, H.-J.; Wang, Z.-H.; Wan, L.-J.; Wang, D. Molecular Evidence for the Intermolecular S···S Interaction in the Surface Molecular Packing Motifs of a Fused Thiophene Derivative. *Chem. Commun.* **2013**, *49*, 1829−1831.

(3) Politzer, P.; Murray, J. S. Halogen Bonding: An Interim Discussion. *ChemPhysChem* **2013**, *14*, 278−294.

(4) Iwaoka, M.; Isozumi, N. Hypervalent Nonbonded Interactions of a Divalent Sulfur Atom. Implications in Protein Architecture and the Functions. *Molecules* **2012**, *17*, 7266−7283.

(5) Sánchez-Sanz, G.; Trujillo, C.; Alkorta, I.; Elguero, J. Intermolecular Weak Interactions in HTeXH Dimers (X = O, S, Se, Te): Hydrogen Bonds, Chalcogen−Chalcogen Contacts and Chiral Discrimination. *ChemPhysChem* **2012**, *13*, 496−503.

(6) Junming, L.; Yunxiang, L.; Subin, Y.; Weiliang, Z. Theoretical and Crystallographic Data Investigations of Noncovalent S···O Interactions. *Struct. Chem.* **2011**, *22*, 757−963.

(7) Bleiholder, C.; Werz, D. B.; Koppel, H.; Gleiter, R. Theoretical Investigations on Chalcogen−Chalcogen Interactions: What Makes These Nonbonded Interactions Bonding? *J. Am. Chem. Soc.* **2006**, *128*, 2666−2674.

(8) Sanz, P.; Mó, O.; Yáñez, M. Characterization of Intramolecular Hydrogen Bonds and Competitive Chalcogen−Chalcogen Interactions on the Basis of the Topology of the Charge Density. *Phys. Chem. Chem. Phys.* **2003**, *5*, 2942−2947.

(9) Sanz, P.; Yáñez, M.; Mó, O. Resonance-Assisted Intramolecular Chalcogen−Chalcogen Interactions? *Chem.—Eur. J.* **2003**, *9*, 4548−4555.

(10) Esseffar, M. H.; Herrero, R.; Quintanilla, E.; Dávalos, J. Z.; Jiménez, P.; Abboud, J.-L. M.; Yáñez, M.; Mó, O. Activation of the Disulfide Bond and Chalcogen−Chalcogen Interactions: An Experimental (FTICR) and Computational Study. *Chem.—Eur. J.* **2007**, *13*, 1796−1803.

(11) Werz, D. B.; Gleiter, R.; Rominger, F. Nanotube Formation Favored by Chalcogen−Chalcogen Interactions. *J. Am. Chem. Soc.* **2002**, *124*, 10638−10639.

(12) Iwaoka, M.; Takemoto, S.; Tomoda, S. Statistical and Theoretical Investigations on the Directionality of Nonbonded S···O Interactions. Implications for Molecular Design and Protein Engineering. *J. Am. Chem. Soc.* **2002**, *124*, 10613−10620.

(13) Nagao, Y.; Hirata, T.; Goto, S.; Sano, S.; Kakehi, A.; Iizuka, K.; Shiro, M. Intramolecular Nonbonded S···O Interaction Recognized in (Acylimino)Thiadiazoline Derivatives as Angiotensin II Receptor Antagonists and Related Compounds. *J. Am. Chem. Soc.* **1998**, *120*, 3104−3110.

(14) Azofra, L. M.; Scheiner, S. Complexation of N SO_2 Molecules (N=1,2,3) with Formaldehyde and Thioformaldehyde. *J. Chem. Phys.* **2014**, *140*, 034302.

(15) Adhikari, U.; Scheiner, S. Sensitivity of Pnicogen, Chalcogen, Halogen and H-Bonds to Angular Distortions. *Chem. Phys. Lett.* **2012**, *532*, 31−35.

(16) Evangelisti, L.; Feng, G.; Gou, Q.; Grabow, J.-U.; Caminati, W. Halogen Bond and Free Internal Rotation: The Microwave Spectrum of CF_3Cl−Dimethyl Ether. *J. Phys. Chem. A* **2014**, *118*, 579−582.

(17) Hauchecorne, D.; Herrebout, W. A. Experimental Characterization of C−X···Y−C (X = Br, I; Y = F, Cl) Halogen−Halogen Bonds. *J. Phys. Chem. A* **2013**, *117*, 11548−11557.

(18) Riley, K. E.; Murray, J. S.; Fanfrlík, J.; Rezác, J.; Solá, R. J.; Concha, M. C.; Ramos, F. M.; Politzer, P. Halogen Bond Tunability II: The Varying Roles of Electrostatic and Dispersion Contributions to Attraction in Halogen Bonds. *J. Mol. Model.* **2013**, *19*, 4651−4659.

(19) Vener, M. V.; Shishkina, A. V.; Rykounov, A. A.; Tsirelson, V. G. Cl···Cl Interactions in Molecular Crystals: Insights from the Theoretical Charge Density Analysis. *J. Phys. Chem. A* **2013**, *117*, 8459−8467.

(20) Solimannejad, M.; Malekani, M. Substituent Effects on the Cooperativity of Halogen Bonding. *J. Phys. Chem. A* **2013**, *117*, 5551−5557.

(21) Stone, A. J. Are Halogen Bonded Structures Electrostatically Driven? *J. Am. Chem. Soc.* **2013**, *135*, 7005−7009.

(22) Erdelyi, M. Halogen Bonding in Solution. *Chem. Soc. Rev.* **2012**, *41*, 3547−3557.

(23) Legon, A. C. The Halogen Bond: An Interim Perspective. *Phys. Chem. Chem. Phys.* **2010**, *12*, 7736−7747.

(24) Auffinger, P.; Hays, F. A.; Westhof, E.; Ho, P. S. Halogen Bonds in Biological Molecules. *Proc. Nat. Acad. Sci., U.S.A.* **2004**, *101*, 16789−16794.

(25) Scheiner, S. Sensitivity of Noncovalent Bonds to Intermolecular Separation: Hydrogen, Halogen, Chalcogen, and Pnicogen Bonds. *CrystEngComm* **2013**, *15*, 3119−3124.

(26) Alkorta, I.; Elguero, J.; Del Bene, J. E. Pnicogen-Bonded Cyclic Trimers $(PH_2X)_3$ with X = F, Cl, OH, NC, CN, CH_3, H, and BH_2. *J. Phys. Chem. A* **2013**, *117*, 4981−4987.

(27) Sánchez-Sanz, G.; Alkorta, I.; Trujillo, C.; Elguero, J. Intramolecular Pnicogen Interactions in PHF-$(CH_2)_n$-PHF (n=2−6) Systems. *ChemPhysChem* **2013**, *14*, 1656−1665.

(28) Liu, X.; Cheng, J.; Li, Q.; Li, W. Competition of Hydrogen, Halogen, and Pnicogen Bonds in the Complexes of HArF with XH_2P (X = F, Cl, and Br). *Spectrochim. Acta, Part A* **2013**, *101*, 172−177.

(29) Bühl, M.; Kilian, P.; Woollins, J. D. Prediction of a New Delocalised Bonding Motif between Group 15 or Group 16 Atoms. *ChemPhysChem* **2011**, *12*, 2405−2408.

(30) Zahn, S.; Frank, R.; Hey-Hawkins, E.; Kirchner, B. Pnicogen Bonds: A New Molecular Linker? *Chem.—Eur. J.* **2011**, *17*, 6034−6038.
(31) Moilanen, J.; Ganesamoorthy, C.; Balakrishna, M. S.; Tuononen, H. M. Weak Interactions between Trivalent Pnictogen Centers: Computational Analysis of Bonding in Dimers $X_3E\cdots EX_3$ (E = Pnictogen, X = Halogen). *Inorg. Chem.* **2009**, *48*, 6740−6747.
(32) Scheiner, S. The Pnicogen Bond: Its Relation to Hydrogen, Halogen, and Other Noncovalent Bonds. *Acc. Chem. Res.* **2013**, *46*, 280−288.
(33) Adhikari, U.; Scheiner, S. Effects of Carbon Chain Substituent on the P···N Noncovalent Bond. *Chem. Phys. Lett.* **2012**, *536*, 30−33.
(34) Scheiner, S. Effects of Substituents upon the P···N Noncovalent Interaction: The Limits of Its Strength. *J. Phys. Chem. A* **2011**, *115*, 11202−11209.
(35) Scheiner, S. A New Noncovalent Force: Comparison of P···N Interaction with Hydrogen and Halogen Bonds. *J. Chem. Phys.* **2011**, *134*, 094315.
(36) Adhikari, U.; Scheiner, S. The S···N Noncovalent Interaction: Comparison with Hydrogen and Halogen Bonds. *Chem. Phys. Lett.* **2011**, *514*, 36−39.
(37) Scheiner, S.; Adhikari, U. Abilities of Different Electron Donors (D) to Engage in a P···D Noncovalent Interaction. *J. Phys. Chem. A* **2011**, *115*, 11101−11110.
(38) Scheiner, S. Weak H-Bonds. Comparisons of CH···O to NH···O in Proteins and PH···N to Direct P···N Interactions. *Phys. Chem. Chem. Phys.* **2011**, *13*, 13860−13872.
(39) Adhikari, U.; Scheiner, S. Preferred Configurations of Peptide−Peptide Interactions. *J. Phys. Chem. A* **2013**, *117*, 489−496.
(40) Adhikari, U.; Scheiner, S. Substituent Effects on Cl···N, S···N, and P···N Noncovalent Bonds. *J. Phys. Chem. A* **2012**, *116*, 3487−3497.
(41) Gronert, S. Theoretical Studies of Proton Transfers. 1. The Potential Energy Surfaces of the Identity Reactions of the First- and Second-Row Non-Metal Hydrides with Their Conjugate Bases. *J. Am. Chem. Soc.* **1993**, *115*, 10258−10266.
(42) Meot-Ner, M. The Ionic Hydrogen Bond and Ion Solvation. 1. $NH^+\cdots O$, $NH^+\cdots N$, and $OH^+\cdots O$ Bonds. Correlations with Proton Affinity. Deviations Due to Structural Effects. *J. Am. Chem. Soc.* **1984**, *106*, 1257−1264.
(43) Meot-Ner, M.; Sieck, L. W. The Ionic Hydrogen Bond and Ion Solvation. 5. $OH\cdots O^-$ Bonds. Gas Phase Solvation and Clustering of Alkoxide and Carboxylate Anions. *J. Am. Chem. Soc.* **1986**, *108*, 7525−7529.
(44) Horowitz, S.; Dirk, L. M. A.; Yesselman, J. D.; Nimtz, J. S.; Adhikari, U.; Mehl, R. A.; Scheiner, S.; Houtz, R. L.; Al-Hashimi, H. M.; Trievel, R. C. Conservation and Functional Importance of Carbon−Oxygen Hydrogen Bonding in Adomet-Dependent Methyltransferases. *J. Am. Chem. Soc.* **2013**, *135*, 15536−15548.
(45) Adhikari, U.; Scheiner, S. The Magnitude and Mechanism of Charge Enhancement of CH··O H-Bonds. *J. Phys. Chem. A* **2013**, *117*, 10551−10562.
(46) Beyeh, N. K.; Cetina, M.; Rissanen, K. Halogen Bonded Analogues of Deep Cavity Cavitands. *Chem. Commun.* **2014**, *50*, 1959−1961.
(47) Rosokha, S. V.; Stern, C. L.; Ritzert, J. T. Experimental and Computational Probes of the Nature of Halogen Bonding: Complexes of Bromine-Containing Molecules with Bromide Anions. *Chem.—Eur. J.* **2013**, *19*, 8774−8788.
(48) Gushchin, P. V.; Kuznetsov, M. L.; Haukka, M.; Kukushkin, V. Y. Recognition of a Novel Type X = N−Hal···Hal (X = C, S, P; Hal = F, Cl, Br, I) Halogen Bonding. *J. Phys. Chem. A* **2013**, *117*, 2827−2834.
(49) Sarwar, M. G.; Dragisic, B.; Dimitrijevic, E.; Taylor, M. S. Halogen Bonding between Anions and Iodoperfluoroorganics: Solution-Phase Thermodynamics and Multidentate-Receptor Design. *Chem.—Eur. J.* **2013**, *19*, 2050−2058.
(50) Chudzinski, M. G.; McClary, C. A.; Taylor, M. S. Anion Receptors Composed of Hydrogen- and Halogen-Bond Donor Groups: Modulating Selectivity with Combinations of Distinct Noncovalent Interactions. *J. Am. Chem. Soc.* **2011**, *133*, 10559−10567.
(51) Dimitrijevic, E.; Kvak, O.; Taylor, M. S. Measurements of Weak Halogen Bond Donor Abilities with Tridentate Anion Receptors. *Chem. Commun.* **2010**, *466*, 9025−9027.
(52) Zhang, Y. On the Role of Halogen Bond in the Halophilic Reaction: A Theoretical Study. *J. Mol. Struct.: THEOCHEM* **2010**, *961*, 6−8.
(53) Deepa, P.; Pandiyan, B. V.; Kolandaivel, P.; Hobza, P. Halogen Bonds in Crystal TTF Derivatives: An Ab Initio Quantum Mechanical Study. *Phys. Chem. Chem. Phys.* **2014**, *16*, 2038−2047.
(54) Zhang, Y.; Li, A.-Y.; Cao, L.-J. Electronic Properties of the Halogen Bonds $Z_3CX\cdots Y^-$ between Halide Anions and Methyl Halides. *Struct. Chem.* **2012**, *23*, 627−636.
(55) Grabowski, S. J. Tetrel Bond−σ-Hole Bond as a Preliminary Stage of the S_N2 Reaction. *Phys. Chem. Chem. Phys.* **2014**, *16*, 1824−1834.
(56) Grabowski, S. J. S-Hole Bond versus Hydrogen Bond: From Tetravalent to Pentavalent N, P, and As Atoms. *Chem.—Eur. J.* **2013**, *19*, 14600−14611.
(57) Han, N.; Zeng, Y.; Li, X.; Zheng, S.; Meng, L. Enhancing Effects of Electron-Withdrawing Groups and Metallic Ions on Halogen Bonding in the $YC_6F_4X\cdots C_2H_8N_2$ (X = Cl, Br, I; Y = F, CN, NO_2, $LINC^+$, $NaNC^+$) Complex. *J. Phys. Chem. A* **2013**, *117*, 12959−12968.
(58) Grabowski, S. J. Cooperativity of Hydrogen and Halogen Bond Interactions. *Theor. Chem. Acc.* **2013**, *132*, 1347.
(59) Alikhani, E.; Fuster, F.; Madebene, B.; Grabowski, S. J. Topological Reaction Sites — Very Strong Chalcogen Bonds. *Phys. Chem. Chem. Phys.* **2014**, *16*, 2430−2442.
(60) Bauzá, A.; Alkorta, I.; Frontera, A.; Elguero, J. On the Reliability of Pure and Hybrid DFT Methods for the Evaluation of Halogen, Chalcogen, and Pnicogen Bonds Involving Anionic and Neutral Electron Donors. *J. Chem. Theory Comput.* **2013**, *9*, 5201−5210.
(61) Frisch, M. J.; Trucks, G. W.; Schlegel, H. B.; Scuseria, G. E.; Robb, M. A.; Cheeseman, J. R.; Scalmani, G.; Barone, V.; Mennucci, B.; Petersson, G. A.; Nakatsuji, H.; Caricato, M.; Li, X.; Hratchian, H. P.; Izmaylov, A. F.; Bloino, J.; Zheng, G.; Sonnenberg, J. L.; Hada, M.; Ehara, M.; Toyota, K.; Fukuda, R.; Hasegawa, J.; Ishida, M.; Nakajima, T.; Honda, Y.; Kitao, O.; Nakai, H.; Vreven, T.; Montgomery, J. A., Jr.; Peralta, J. E.; Ogliaro, F.; Bearpark, M.; Heyd, J. J.; Brothers, E.; Kudin, K. N.; Staroverov, V. N.; Kobayashi, R.; Normand, J.; Raghavachari, K.; Rendell, A.; Burant, J. C.; Iyengar, S. S.; Tomasi, J.; Cossi, M.; Rega, N.; Millam, J. M.; Klene, M.; Knox, J. E.; Cross, J. B.; Bakken, V.; Adamo, C.; Jaramillo, J.; Gomperts, R.; Stratmann, R. E.; Yazyev, O.; Austin, A. J.; Cammi, R.; Pomelli, C.; Ochterski, J. W.; Martin, R. L.; Morokuma, K.; Zakrzewski, V. G.; Voth, G. A.; Salvador, P.; Dannenberg, J. J.; Dapprich, S.; Daniels, A. D.; Farkas, O.; Foresman, J. B.; Ortiz, J. V.; Cioslowski, J.; Fox, D. J. *Gaussian 09*, revision B.01; Gaussian Inc.: Wallingford, CT, 2009.
(62) Zhao, Q.; Feng, D.; Sun, Y.; Hao, J.; Cai, Z. Theoretical Investigations on the Weak Nonbonded $C{=}S\cdots CH_2$ Interactions: Chalcogen-Bonded Complexes with Singlet Carbene as an Electron Donor. *Int. J. Quantum Chem.* **2011**, *111*, 3881−3887.
(63) Wu, J. Structure, Properties, and Nature of the BrF−HX Complexes: An Ab Initio Study. *Int. J. Quantum Chem.* **2011**, *111*, 4247−4254.
(64) Wu, W.; Lu, Y.; Liu, Y.; Li, H.; Peng, C.; Liu, H.; Zhu, W. Weak Energetic Effects between X−P and X−N Halogen Bonds: CSD Search and Theoretical Study. *Chem. Phys. Lett.* **2013**, *582*, 49−55.
(65) Kerdawy, A. E.; Murray, J. S.; Politzer, P.; Bleiziffer, P.; Heßelmann, A.; Görling, A.; Clark, T. Directional Noncovalent Interactions: Repulsion and Dispersion. *J. Chem. Theory Comput.* **2013**, *9*, 2264−2275.
(66) Wu, W.; Zeng, Y.; Li, X.; Zhang, X.; Zheng, S.; Meng, L. Interplay between Halogen Bonds and Hydrogen Bonds in OH/SH···HOX···HY (X = Cl, Br; Y = F, Cl, Br) Complexes. *J. Mol. Model.* **2013**, *19*, 1069−1077.

(67) Ji, W.-Y.; Xia, X.-L.; Ren, X.-H.; Wang, F.; Wang, H.-J.; Diao, K.-S. The Non-Covalent Bindings of CF_2Cl_2 with NO and SO_2. *Struct. Chem.* **2013**, *24*, 49−54.
(68) Georg, H. C.; Fileti, E. E.; Malaspina, T. Ab Initio Study of Weakly Bound Halogen Complexes: RX···PH_3. *J. Mol. Model.* **2013**, *19*, 329−336.
(69) Li, H.; Lu, Y.; Liu, Y.; Zhu, X.; Liu, H.; Zhu, W. Interplay between Halogen Bonds and $\pi-\pi$ Stacking Interactions: CSD Search and Theoretical Study. *Phys. Chem. Chem. Phys.* **2012**, *14*, 9948−9955.
(70) Boys, S. F.; Bernardi, F. The Calculation of Small Molecular Interactions by the Differences of Separate Total Energies. Some Procedures with Reduced Errors. *Mol. Phys.* **1970**, *19*, 553−566.
(71) Reed, A. E.; Curtiss, L. A.; Weinhold, F. Intermolecular Interactions from a Natural Bond Orbital, Donor−Acceptor Viewpoint. *Chem. Rev.* **1988**, *88*, 899−926.
(72) Reed, A. E.; Weinhold, F.; Curtiss, L. A.; Pochatko, D. J. Natural Bond Orbital Analysis of Molecular Interactions: Theoretical Studies of Binary Complexes of HF, H_2O, NH_3, N_2, O_2, F_2, CO and CO_2 with HF, H_2O, and NH_3. *J. Chem. Phys.* **1986**, *84*, 5687−5705.
(73) Moszynski, R.; Wormer, P. E. S.; Jeziorski, B.; van der Avoird, A. Symmetry-Adapted Perturbation Theory of Nonadditive Three-Body Interactions in Van Der Waals Molecules. I. General Theory. *J. Chem. Phys.* **1995**, *103*, 8058−8074.
(74) Werner, H.-J.; Knowles, P. J.; Knizia, G.; Manby, F. R.; Schütz, M.; Celani, P.; Korona, T.; Lindh, R.; Mitrushenkov, A.; Rauhut, G.; Shamasundar, K. R.; Adler, T. B.; Amos, R. D.; Bernhardsson, A.; Berning, A.; Cooper, D. L.; Deegan, M. J. O.; Dobbyn, A. J.; Eckert, F.; Goll, E.; Hampel, C.; Hesselmann, A.; Hetzer, G.; Hrenar, T.; Jansen, G.; Köppl, C.; Liu, Y.; Lloyd, A. W.; Mata, R. A.; May, A. J.; McNicholas, S. J.; Meyer, W.; Mura, M. E.; Nicklass, A.; O'Neill, D. P.; Palmieri, P.; Pflüger, K.; Pitzer, R.; Reiher, M.; Shiozaki, T.; Stoll, H.; Stone, A. J.; Tarron, R.; Thorsteinsson, T.; Wang, M.; Wolf, A. *Molpro*, version 2010.1, a Package of Ab Initio Programs; 2010.